An anisotropic diffusion-based dynamic combined energy model for seismic denoising

Hui Chen[1,2], Ying Hu[1,2], and Kurt. J. Marfurt[2], [1]Chengdu University of Technology; [2]University of Oklahoma

AASPI

The UNIVERSITY of OKLAHOMA
Mewbourne College of Earth and Energy
ConocoPhillips School of Geology and Geophysics
ConocoPhillips

Summary

We combine anisotropic and isotropic diffusion models and establish a combined energy variational model for seismic denoising. For each inline vertical slice, we use a dynamic threshold to separate the seismic data into different features in order to choose a diffusion method based on the local seismic data characteristics. The method automatically handles both noise and discontinuities (edges) at different scales. Denoised results from a synthetic model and from field seismic sections demonstrate that our proposed model can efficiently suppress random noise and preserve edges in seismic data.

Introduction

Noise attenuation is one of the fundamental topics in geophysical data processing and is especially crucial for seismic data interpretation and analysis; consequently, noise attenuation is the focus of many studies (Cai, 2011; Zhou, 2016).

Traditionally, seismic noise is separated from signal using f-k and Radon transforms, time-frequency analysis, deconvolution, and simple stacking (Zhu, 2015; Li, 2014; Canales, 1984). Other special domains have also been introduced for seismic denoising, including the bounded variation (BV) space with the total variation (TV) regularization model (Rudin, 1992; Anagaw, 2012). Less commonly used transforms include wavelet transforms (Gao, 2006), curvelet transforms (Lari, 2014), contourlet transforms (Do, 2005), and seislet transforms (Chen, 2014). In suitable domains, most noise suppression techniques eliminate unwanted noise components by simply setting them to zero before applying an inverse transform (Done, 1991).

A robust noise reduction method known as edge preserving smoothing (EPS) was introduced in 2002, based on the multi-window analysis technique of Kuwahara *et al.* The EPS technique has been utilized in exploration geophysics and has achieved notable success in practice (Luo, 2002; Marfurt, 2002). In addition to the EPS methods, several nonquadratic regularization methods have been developed based upon partial differential equations (PDEs) with the goal of suppressing noise and preserving sharp boundaries in geophysical imaging and during seismic denoising (Sun,2016).

As an alternative to linear filters, Ferahtia et al. (2013) presented two image-based nonlinear filters - the anisotropic nonlinear diffusion filter and the trilateral filter, to enhance the identification of geophysical features and more efficiently remove random and/or coherent noise.

In seismic data, "apparent discontinuities" that occur when noise cuts through otherwise continuous reflectors are often not as strongly defined as real discontinuities that define at faults and stratigraphic edges. Thus, we proposes a combined algorithm for the separation of noise and apparent discontinuities from discontinuities of. Our approach is based on the method presented by Chambolle and Lions (Chambolle, 1997), which utilizes the minimization of several convex functionals of the gradient in a BV space. Similar approaches have been employed previously in medical imaging (Lieu, 2008), but have not yet been applied to seismic denoising. The objective of this paperis to demonstrate the utility of this adaptive combined energy method for seismic denoising.

Principles of Anisotropic diffusion

The anisotropic diffusion equation can be obtained by minimizing the following energy functional:

$$J(u) = \int_\Omega G(|\nabla u|^2)dx \qquad (1)$$

The related partial differential equations can be denoted:

$$\begin{cases} \frac{\partial u}{\partial t} = \mathrm{div}[g(|\nabla u|)\cdot \nabla u] \\ u(x,0) = u_0(x) \end{cases} \qquad (2)$$

When such an anisotropic diffusion equation is applied to remove noise, it generally blurs certain features because of the inconsistent edge. Consequently, Chambolle and Lions proposed their anisotropic diffusion method by minimizing the following hybrid functional:

$$E_{CL}(u) = \frac{1}{2\beta}\int_{|\nabla u|<\beta} |\nabla u|^2 \mathrm{d}x + \int_{|\nabla u|\geq\beta}\left(|\nabla u| - \frac{\beta}{2}\right)\mathrm{d}x \qquad (3)$$

The constant $\beta > 0$ is the threshold of the magnitude of the image gradients $|\nabla u|$. It separates regions containing more features from those with fewer features, similar to distinguishing between features and noise in image-processing techniques, and thus plays an important role in this model.

Dynamic combined energy model

To separate noise and false features from edges and real faults and to subsequently adopt different diffusion methods to treat this separation accordingly, we introduce a dynamic energy based on the CL model.

A dynamic threshold β_f , which is based upon each value of seismic data f , is proposed[(4)] to optimally distinguish the feature regions. Since the difference in the gradient magnitude is used to distinguish noise from edges, we use the average value of the gradient magnitude to define the threshold

$$\beta_f = \rho\frac{\|f\|_{TV}}{\|\nabla f\|_0} \qquad (4)$$

where $\rho \in [0.5\ 1.5]$ is an empirically determined diffusion parameter to adjust the region division according to the strength of the noise. Then the dynamic CL (DCL) model is:

$$\mathcal{E}_\mathcal{D} = \frac{1}{2\beta_f}\sum_{|\nabla f_{i,j}|<\beta_f}|\nabla f_{i,j}|^2 + \sum_{|\nabla f_{i,j}|\geq\beta_f}\left(|\nabla f_{i,j}| - \frac{\beta_f}{2}\right) \qquad (5)$$

To maintain the stability of the seismic energy and the gradient energy, $\sum_{i,j}|\nabla f_{i,j} - \nabla\hat{f}_{i,j}|^2$ and $\sum_{i,j}(f_{i,j} - \hat{f}_{i,j})^2$ are introduced as constraint parameters to denote the difference between the result f and the initial data $\hat{f}$.

With the Lagrangian multiplier method, these constraints are combined into the DCL model, and an unconstrained optimization problem is obtained. The consequent DCE model can be expressed explicitly as follows:

$$\mathcal{E}_{\mathcal{DE}} = \frac{1}{2\beta_f}\sum_{|\nabla f_{i,j}|<\beta_f}|\nabla f_{i,j}|^2 + \sum_{|\nabla f_{i,j}|\geq\beta_f}\left(|\nabla f_{i,j}| - \frac{\beta_f}{2}\right) + \frac{\gamma}{2}\sum_{i,j}(f_{i,j} - \hat{f}_{i,j})^2 + \frac{\mu}{2}\sum_{i,j}|\nabla f_{i,j} - \nabla\hat{f}_{i,j}|^2 \qquad (6)$$

Minimizing the functional in equation [(6)], anisotropic diffusion can be governed by the following evolution equation:

$$\left[\frac{\partial\mathcal{E}_{\mathcal{DE}}}{\partial f}\right]_{i,j} = \left[\frac{\partial\mathcal{E}_\mathcal{D}}{\partial f}\right]_{i,j} - \gamma(f_{i,j} - \hat{f}_{i,j}) + \mu(\Delta f_{i,j} - \Delta\hat{f}_{i,j}) \qquad (7)$$

Synthetic Examples

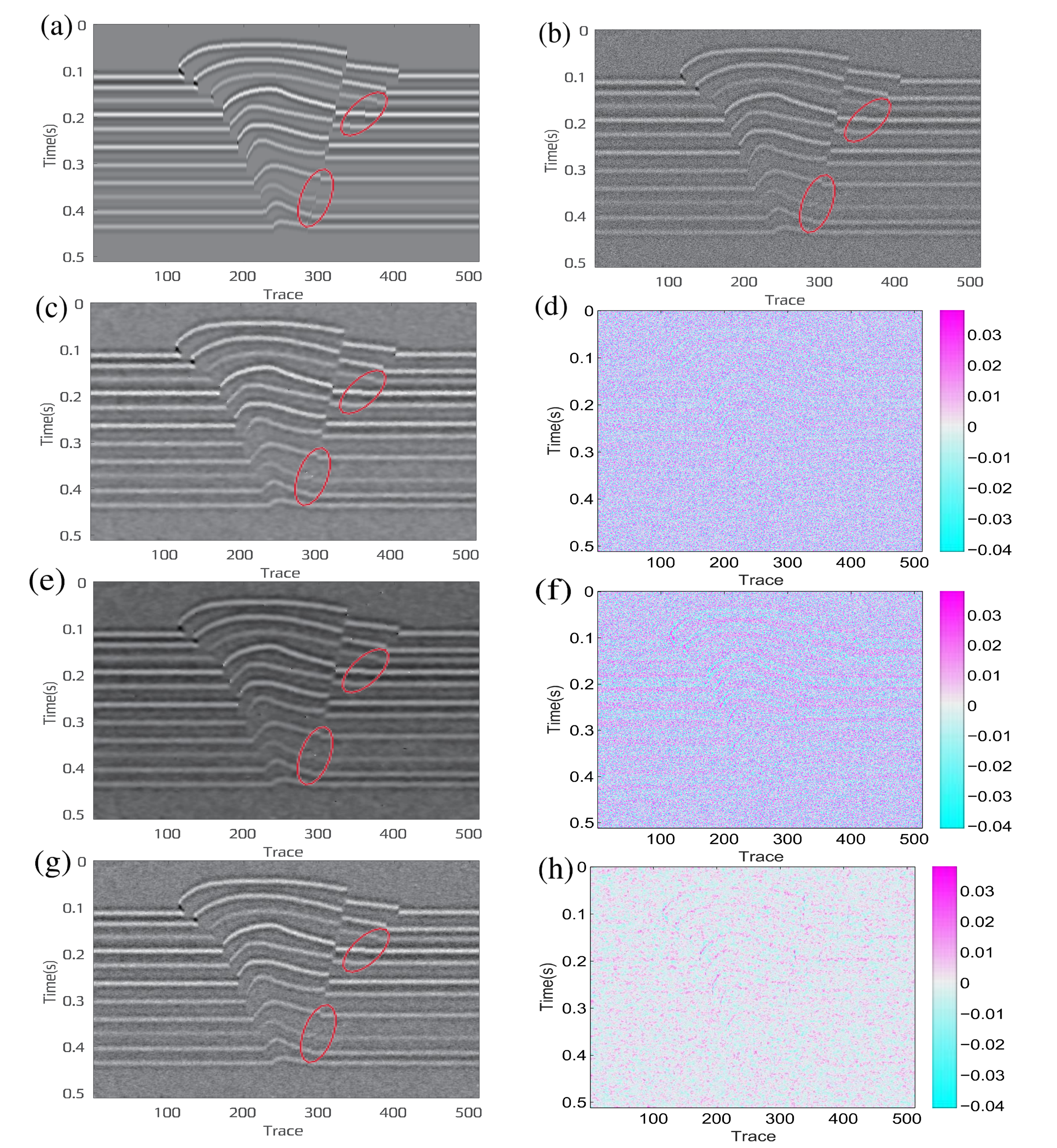

Fig. 1. Synthetic seismic section (a) without and (b) with -3 dB random noise. Filtered data using the (c) DCE, (e) CL (g) TV models. Rejected noise using the (d) DCE, (f) CL (h) TV models.

Table 1 Statistics Regarding the Experiments

Original		TV				Classical CL				DCE			
SNR	SSIM	SNR	SSIM	Iter	Time(s)	SNR	SSIM	Iter	Time(s)	SNR	SSIM	Iter	Time(s)
5	0.8719	10.6898	0.9804	100	7.619772	11.3373	0.9843	13	1.761432	**16.3988**	**0.9885**	**8**	**1.215389**
3	0.8154	9.0239	0.9708	100	7.735348	9.7740	0.9831	**11**	**1.599523**	**15.2126**	**0.9849**	**11**	1.792413
0	0.7068	5.6363	0.9485	100	7.747369	5.9220	0.9716	15	**2.036529**	**13.1474**	**0.9760**	**14**	2.111120
-3	0.5791	2.5017	0.9111	100	7.682360	2.9254	0.9555	26	3.410565	**11.3446**	**0.9635**	**18**	**2.577731**
-5	0.4882	0.1619	0.8722	100	7.715514	-0.9923	0.9383	34	4.397188	**9.7472**	**0.9492**	**25**	**3.738860**
-10	0.2985	-3.8098	0.7379	100	7.944538	-4.8402	0.8536	**42**	**6.063340**	**5.9021**	**0.8826**	**42**	6.404884

Figure 1a shows the noise-free synthetic seismic section, within which the input data include strata with variable thicknesses, seismic reflection events with different amplitudes, and faults with different displacements, which increase from the bottom toward the top, to test the efficiency of each denoising method. Figure 1b shows the same seismic section with -3 dB Gaussian noise where red ellipses show that faults that are masked by the existence of random noise.

Figure 1c illustrates the results of our DCE model, from which we can see that the proposed model smooths the seismic section and preserves the features of the faults well. We can observe that the stronger discontinuities are preserved while the continuity of the weaker reflections are enhanced, thereby substantially improving the quality of the seismic profiles. Examining the residuals of the three filters in Figures 1d, 1f, and 1h, shows that the DCE model better preserves the fault discontinuities. In contrast, the results obtained using the competing CL and TV models reveal that the circled faults are masked with noise even after denoising the data using those methods.

The statistics acquired from other synthetic experiments at other noise levels are shown in Table I, in which we provide the SNRs, SSIMs, iteration numbers, and computation times for all the three denoising methods. From the table, we can observe that using our denoising model, the SNR increases from −3 to 11.3446 dB and the SSIM increases from 0.5791 to 0.9635. Meanwhile, the SNR and SSIM values obtained using the classical CL result are 2.9254 and 0.9555, respectively, and the same respective values obtained from using the TV model are 2.5017 and 0.9111. In addition, we calculated that the SSIM value of trace 380 increased from 0.5945 to 0.9685 for the denoised result.

This synthetic suggests that the proposed method can be used to efficiently remove noise from seismic data while simultaneously enhancing the continuity of the reflection events and preserving the effective discontinuity information and amplitude characteristics in the seismic section.

Field Data Examples

We further verify the effectiveness of the proposed denoising approach by applying the DCE model to two substantially noise-contaminated real seismic sections from Sichuan Basin, China. Figure 2a is a P-wave seismic section while Figure 3a is the corresponding converted-wave (P-SV) seismic section. In these two sections, we can observe that the amplitudes of the reflection events are weak and not obviously continuous, and they cannot be identified effectively since they are obscured by strong incoherent noise.

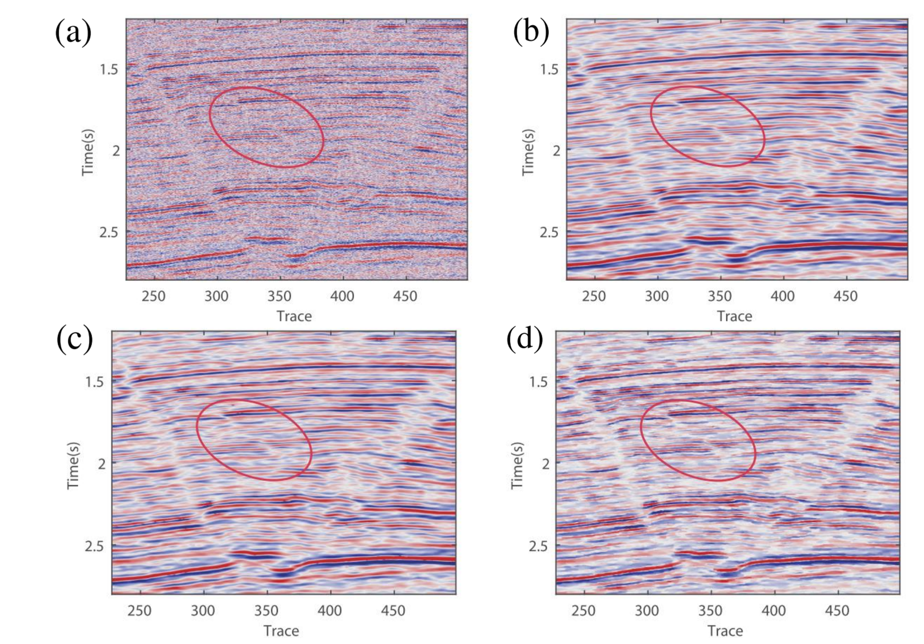

Fig. 2. (a) Original P-P seismic section and denoised results using the (b) DCE (c) CL and (d) TV models.

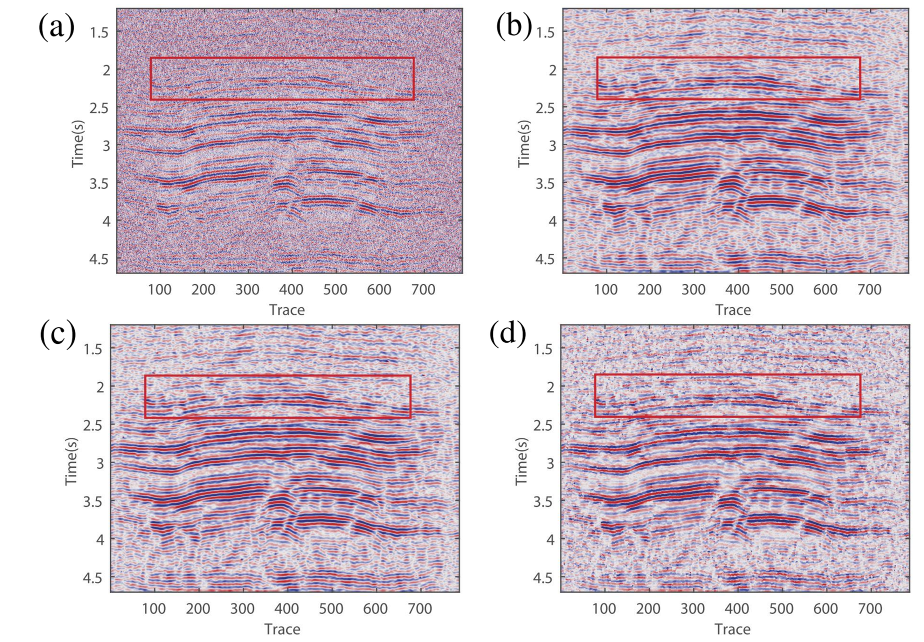

Fig. 3. (a) Original P-SV seismic section and denoised results using the (b) DCE (c) CL and (d) TV models.

After applying our proposed DCE method, we acquire the denoised results Illustrated in Figures 2b and 3b. In these results, the continuity of the seismic events is enhanced, the discontinuities are clearer, and the fault boundaries and displacements are more distinct. The number of iterations is determined using the empirical iteration number from the synthetic model.

The results of the classical CL are shown in Figures 2c and 3c, whereas those of the TV model are depicted in Figures 2d and 3d. Note that the denoising efficacies of the DCE, CL, and TV models appear quite similar. However, although the DCE model removed a significant quantity of random noise, it also preserved more useful signal, while faults previously masked by noise are more clearly enhanced, particularly in indicated by the red ellipses. Similarly, the continuity of the seismic reflections with weak amplitudes that were masked by incoherent noise is also more enhanced, as is illustrated by the encircled area in Figure 3b.

Acknowledgment

Thanks to all sponsors of AASPI consortium group for their generous sponsorship, and Chengdu University of Technology for supporting our visiting scholar positions.